Journal of Chromatography A 1645 (2021) 462103

Contents lists available at ScienceDirect

Journal of Chromatography A

journal homepage: www.elsevier.com/locate/chroma

# Unraveling the Complex Olefin Isomer Mixture Using Two-Dimensional Gas Chromatography-Photoionization-Time of Flight Mass Spectrometry

Yun Zou[a,*], Pierre-Hugues Stefanuto[a], Mariarosa Maimone[b], Marcel Janssen[b], Jean-François Focant[a]

[a] Organic and biological analytical chemistry group, MolSys Research Unit, University of Liège, Allée du 6 aout, B6c, B-4000 Liège Sart Tilman, Belgium
[b] ExxonMobil Chemical Europe Inc., Hermeslaan 2, 1831 Machelen, Belgium

ARTICLE INFO

*Article history:*
Received 13 January 2021
Revised 19 March 2021
Accepted 21 March 2021
Available online 26 March 2021

*Keywords:*
Alkene
GC×GC
Retention index
Branching index
Mass spectra interpretation
Soft ionization

ABSTRACT

Commercial dodecenes are a complex chemical mixture with a majority of $C_{12}$ olefins and minority of $C_{8\text{-}18}$ olefins. Structurally, dodecene products may consist of straight-chain alkenes, branched alkenes, as well as cyclic hydrocarbons. Due to the difference of feeds and catalysts used in the oligomerization reaction, the composition of the dodecenes is complex and their properties are very different. Knowing the complex composition of dodecenes can help tune the production process and select the appropriate products according to their end use. To reveal the complex profile of dodecenes, an analytical method using two-dimensional gas chromatography (GC×GC) coupled photoionization (PI) - time of flight mass spectrometry (TOFMS) was developed in this study. A conventional (nonpolar × polar) column combination (non-polar column as 1st dimension and mid-polar column as 2nd dimension) was selected. The analytical condition of GC was optimized using fractional factorial experimental design (DoE). Olefin congener grouping by carbon chain length and double bond equivalent (DBE) was achieved based on the detection of molecular ions by PI-TOFMS. Grouping of dodecenes by linear, mono-branched, di- and tri-branched subgroups was achieved based on branching index (BI) under the assumption of no retention time (RT) overlap among subgroups. Certain dodecene isomers were identified by retention index (RI) and further confirmed by PI mass spectra. The information altogether provided a multimodal characterization possibility to be used with statistical tools. Principal component analysis (PCA) and hierarchical clustering analysis (HCA) of seventeen dodecene samples explained the composition variance between catalysts solid phosphoric acid and zeolite, as well as between feeds with $C_4$ and without $C_4$.



## 1. Introduction

Commercial dodecenes are petrochemical mixtures used to manufacture products applied in lube oil additives and surfactants, and also be used as feedstocks for alcohols. They are defined as olefinic hydrocarbons boiling between 185 and 205 °C produced by oligomerization of $C_3$ and $C_4$ olefins. Some dodecene products are manufactured during nonene recycle (NR). A variety of catalysts, such as solid phosphoric acid and zeolites, were applied in oligomerization process [1]. Commercial dodecens are actually complex olefin congener and isomer mixtures with a majority of $C_{12}$ olefins and a wide range of $C_{8\text{-}18}$ olefins as minority. Structurally they may consist of linear alkenes (*n*-alkenes or *n*-olefins), branched alkenes (*iso*-alkenes or *iso*-olefins), as well as cyclic hydrocarbons. Due to the difference of feeds and catalysts used in the oligomerization reaction, the composition of the dodecenes is complex and their properties are very different. Knowing the complex composition of dodecenes can help tune the production process and select the appropriate dodecenes according to their end use. However, to comprehensively understand the composition of olefin mixtures has been a challenge due to the extraordinary complexity of the object.

Two-dimensional gas chromatography (GC×GC) has been extensively applied for revealing the composition of complex mixtures of volatile organic compounds (VOCs) and semi-volatile organic compounds (SVOCs) in petrochemical industry [2–4]. It is because of the enhanced separation power and informative structural

* Corresponding author.
*E-mail addresses:* yun.zou.titech@gmail.com, yun_zou_titech@163.com (Y. Zou), phstefanuto@uliege.be (P.-H. Stefanuto), mariarosa.maimone@exxonmobil.com (M. Maimone), marcel.j.janssen@exxonmobil.com (M. Janssen), JF.Focant@uliege.be (J.-F. Focant).

https://doi.org/10.1016/j.chroma.2021.462103
0021-9673/

elution pattern offered by GC×GC compared with one-dimensional (1D) GC. Time of flight mass spectrometry (TOFMS) is commonly coupling to GC×GC because of its high spectrum acquisition speed and no spectral skewing [2–5]. Standard electron ionization (EI) with electrons possessing 70 eV of kinetic energy is the most common ionization technique for GC-MS. The fragmentation patterns can be used to identify the chemicals by comparing with mass spectral libraries. However, such high energy causes nonspecific fragmentation pattern with very low or even without signals of molecular ions for straight and branched paraffins and olefins. For this reason, structural identification of same classes of chemicals, such as olefins in this study, can be hindered by EI mass spectra [6]. In contrast, soft ionization techniques such as cold EI [7], chemical ionization (CI) [8–10], field ionization (FI) [11–13], and photoionization (PI) [14,15], all produce little or no fragmentation with significantly enhanced molecular ion signals. Giri and co-workers [2,5] evaluated GC×GC-PI-TOFMS performance on petroleum base oils and demonstrated that the superior separation and valuable mass spectra retaining significant molecular ion information and unique fragmentation patterns enabled effective isomeric identification of hydrocarbons, particularly branched alkanes and cycloalkanes.

There are researches attempting to disentangle the olefin mixture "puzzle" and identify isomer structures using 1D-GC-EI-MS [16,17] and photodissociation-photoionization MS (PDPI-MS) [18–21]. However, the olefins studied previously were either *n*-alkenes or *iso*-alkenes with carbon chain length not longer than 8. Co-elution on 1D-GC together with lacking of olefin isomer references hampered isomeric identification [22]. Moreover, the number of isomers increases exponentially with addition of carbon number. To be specific, Bekker and co-workers detected 93 isomers of octene, whereas dodecene has 3226 isomers [22], making separation and identification extra difficult. Although GC×GC has been applied in olefin identification [4,23], it is limited to the level of carbon chain length; isomeric identification has not been achieved yet. Therefore, the goal of this study is to evaluate the applicability of state-of-the art GC×GC-PI-TOFMS on molecular structural characterization of complex mixtures of olefins. An analytical method was developed and the structural composition of commercial dodecene products was obtained. First, olefin congener grouping by carbon chain length and double bond equivalent (DBE, calculated from valence values of elements contained in the formula, e.g. an element with $x$ valence contributes with $x - 2$ to the DBE value) were achieved based on the enhanced signal of molecular ions by PI. Second, the subgroups distribution, including linear, mono-branched, di- and tri-branched dodecene isomers, were calculated under the assumption of no overlap on retention time in the 1$^{st}$ dimension ($^1t_R$). Third, the structures of certain dodecene isomers were predicted by retention index (RI) and confirmed by PI mass spectra. Finally, a statistical analysis based on the global information of dodecenes revealed that the variance of dodecene products was caused by different feeds and catalysts.

## 2. Material and methods

### 2.1. Chemicals and Samples

1-dodecene and 1-tetradecene standards purchased from Chevron Phillips Chemical Company (TX, U.S.A.) were used to evaluate PI mass spectra. The branching index (BI) reference sample (BI-reference-sample hereinafter) provided by ExxonMobil (Machelen, Belgium) were used to estimate $^1t_R$ boundary of subgroups (linear, mono-branched, di- and tri-branched) of dodecene and to predict isomer structures. Seventeen dodecene products, namely Samples A – Q, representing two types of catalysts and four types of feeds were collected (Table S1) and calculated for the percent distribution of olefin congener groups and dodecene subgroups by weight (% w/w). The two catalysts used were zeolite and solid phosphoric acid, which are commercially available from reputable vendors. Four types of feeds were short chain olefins and mixtures thereof, $C_3$, $C_4$, $C_3$+$C_4$, and $C_3$+$C_9$. All the feeds are either commercial refinery grade olefins or purchased from Air Liquide. In addition, the exact feed composition for Samples P and Q were unknown. Samples A – Q were prepared under typical oligomerization conditions, which is 180 °C and 65 bar pressure, and then obtained by distillation in the temperature range of 185 – 215 °C. Sample Q was used for analytical condition optimization because that it contained the widest carbon chain length ($C_{9\text{-}18}$) distribution among the seventeen dodecene samples evaluated. A $C_{7\text{-}30}$ *n*-alkane mixture used for Kovats' RI calculation was purchased from Millipore Sigma (Bellefonte, PA, U.S.A.). The *n*-hexane (Dioxin and PCB grade, Biosolve, Dieuze, France) was used as dilution solvent.

### 2.2. GC×GC-TOFMS instrumentation

The instrumental analyses were conducted on a GC (7890B, Agilent Technologies, Wilmington, DE, U.S.A.) equipped with a solid-state modulator (SSM1800, J&X technologies, Shanghai, China). A TOFMS with a PI ion source (JMS-T200GC "AccuTOF GCx-plus", JEOL Ltd., Tokyo, Japan) was coupled to GC×GC. The PI was a strictly single-photon photo-ionization with maximum energy output of 10.78 eV at 118 nm. A technical introduction to PI was described elsewhere [2]. Two column sets were examined. In a conventional (nonpolar × polar) column set, the first dimension ($^1$D) column was a non-polar Rxi-5MS (30 m × 0.25 mm i.d. × 0.25 $\mu$m $d_f$, Restek Corporation). The second dimension ($^2$D) column was a mid-polar Rxi-17Sil MS (2 m × 0.25 mm i.d. × 0.25 $\mu$m $d_f$, Restek Corporation). In a reversed (polar × nonpolar) column set, the $^1$D column was Rxi-17Sil MS (60 m × 0.25 mm i.d. × 0.25 $\mu$m $d_f$, Restek Corporation). The $^2$D column was Rxi-5MS (1 m × 0.25 mm i.d. × 0.25 $\mu$m $d_f$, Restek Corporation). A 30 m Rxi-17Sil MS column was also tested as the $^1$D column of the reversed (polar × nonpolar) column set in the preliminary study. However, the 60 m column outperformed the 30 m one on the $^1$D separation power (data not shown). Therefore, the 60 m Rxi-17Sil MS column was employed in the reversed (polar × nonpolar) column set for comparison. Data acquisition was controlled on msAxel ver. 2.1 (JEOL Ltd.). Solid-state modulator was controlled by SSCenter ver. 1.0.12.0 (J&X technologies). The 2D chromatographic space occupations using both column sets were optimized individually based on temperature ramp, carrier gas flow rate, initial oven temperature (for conventional (nonpolar × polar) column set), and dilution ratio (for reversed (polar × nonpolar) column set). The experimental design (DoE) was generated and evaluated using Ellistat ver. 5.29 (Ellistat, Chavanod, France). Both column sets under their respective optimized conditions were capable on congener level separation. The conventional (nonpolar × polar) column set was selected finally due to better separation on isomer level. The optimized condition was as follows. The carrier gas was helium, and flow rate was 0.8 mL/min. The injector temperature was 280 °C. GC oven was set initially at 35 °C, and ramped to final temperature of 140 °C (hold for 1 min) at a rate of 1 °C/min. Interface and ion source temperature were 200 °C and 300 °C, respectively. A mass range of *m/z* 29-450 was collected with an acquisition rate of 50 spectra/s. Daily tuning was performed using toluene. The modulation period ($P_M$) was 4 s. Details about analytical condition were listed in Table S2. The GC×GC data were processed using GC Image ver. 2.5 (Zoex Corporation, Houston, U.S.A.). A Pegasus 4D (Leco Corporation, St. Joseph, MI, U.S.A.) GC×GC-EI-TOFMS instrument equipped with flow modulator and conventional (nonpolar × polar) column set was used to compare EI with PI mass spectra. The configuration was as same as GC×GC-PI-TOFMS. The only difference was $^2$D col-

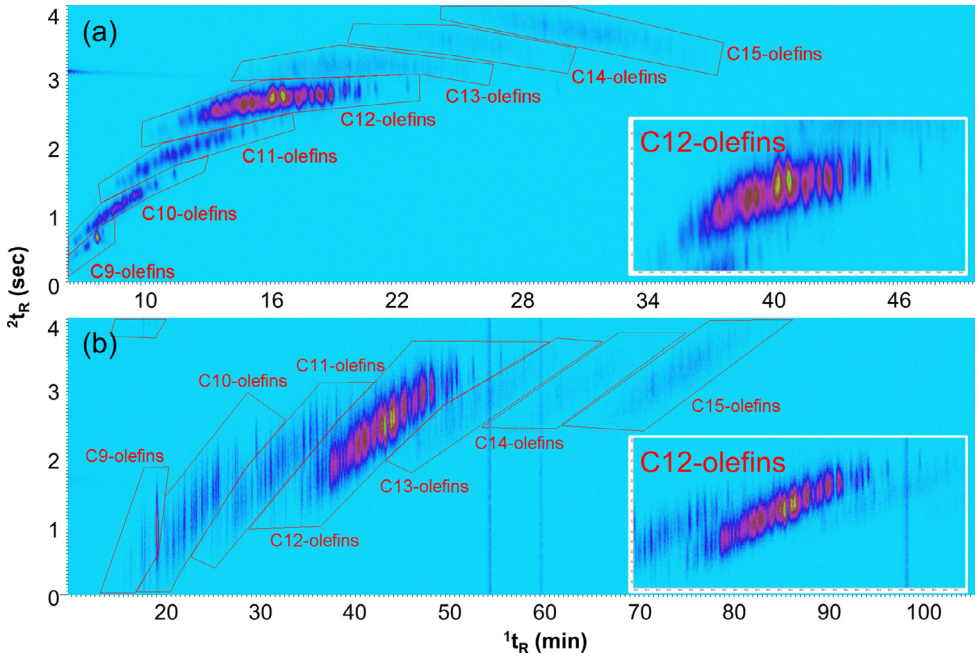


**Fig. 1.** 2D chromatogram comparison between reversed (polar × nonpolar) column set (a) and conventional (nonpolar × polar) column set (b) under respective optimized conditions. The dodecene product used for generating chromatograms was Sample Q.

umn length of 1.4 m instead of 2 m. EI was 70 eV. Data processing of GC×GC-EI-TOFMS was performed on ChromaTOF ver. 4.72 (Leco Corporation).

### 2.3. Hydro GC-FID instrumentation

Hydro GC-FID was applied to examine the existence of cyclic hydrocarbons and to determine BI. An Agilent GC (8890, Agilent Technologies, Wilmington, DE, U.S.A.) was equipped with a Pona column (100 m × 0.25 mm i.d. × 0.5 $\mu$m $d_f$, Sigma Aldrich) and a flame ionization detector (FID). The liner (5062-3587, Agilent Technologies) was filled with deactivated wool. The catalyst located in the inlet of GC was a platinum (Pt) on alumina with 0.5 wt% loading, and it was purchased from Sigma Aldrich (Millipore Sigma, PA, U.S.A.). Details on the configuration are given in Table S3.

### 2.4. Statistical Analysis

Analysis of variance (ANOVA), principle component analysis (PCA), hierarchical clustering analysis (HCA), and heat maps were carried out by R ver. 4.0.2 (R Foundation for Statistical Computing, Vienna, Austria). The raw data were transformed for normality by Log10 calculation for ANOVA. The data pretreatment on the raw data involved autoscaling for plotting heat map and HCA.

## 3. Results and discussion

### 3.1. Optimization of GC×GC separation

To achieve the best separation, both conventional (nonpolar × polar) and reversed (polar × nonpolar) column sets were examined. Sample Q was chosen for condition optimization as described in Section 2.1. A three factor (temperature ramp, carrier gas flow rate, initial oven temperature)-three level fractional factorial DoE was conducted for reversed (polar × nonpolar) column set (Table S4). The main effect plots showed that temperature ramp and flow rate had positive impact on the total peak intensity; while no factor had significant impact on $^1$D resolution ($^1R_s$) of two adjacent peaks (two dodecene isomers) (Fig. S1). With the conventional (nonpolar × polar) column set, the dilution ratio instead of initial oven temperature was chosen as a factor (Table S5). The dilution ratio was the only factor that had a positive effect on the total peak intensity; while no factor had significant impact on $^1R_s$ (Fig. S2). More details regarding DoE results were shown in SI S-3. The optimized conditions for both column sets were shown in Table S2.

The 2D chromatograms of the two column sets under their respective optimized conditions are shown in Fig. 1. Olefin congeners according to carbon chain length were well separated in both column sets. As seen from the expanded chromatograms of $C_{12}$-olefins (see inset), a rather better $^1$D separation was achieved by the conventional (nonpolar × polar) column set. At the meanwhile, $^2$D separation was comparable to the reversed (polar × nonpolar) set. Therefore, the conventional (nonpolar × polar) column set and its optimized condition were applied for further measurements.

### 3.2. Comparison of EI and PI mass spectra of 1-alkenes

EI is known as a hard ionization that produces high intensity of fragments with low or missing signal of molecular ions for most aliphatic hydrocarbons. Unsurprisingly, the EI mass spectra of 1-dodecene and 1-tetradecene showed similar pattern of fragments. The fragmentation was the successive loss of $C_2H_4$ (*m/z* 28). The interval of *m/z* 14 presented in the mass spectra was due to the multiple fragments of the primary chain. The molecular ion intensity was very low or not present (Fig. 2). Contrarily, in the PI mass spectra the highest intensity of 1-alkenes was the molecular ion. Giri and co-workers reported that other chemical classes, such as *n*-alkanes, ketones, fatty acid methyl esters (FAMEs), monoaromatic alkyl benzenes, and polyaromatic hydrocarbons also showed molecular ions as the base peaks in PI mass spectra [2]. This, of course, is a useful feature for grouping congeners which have the same mass weight within the same chemical classes (such as olefins in this study). 1-dodecene and 1-tetradecene, moreover,

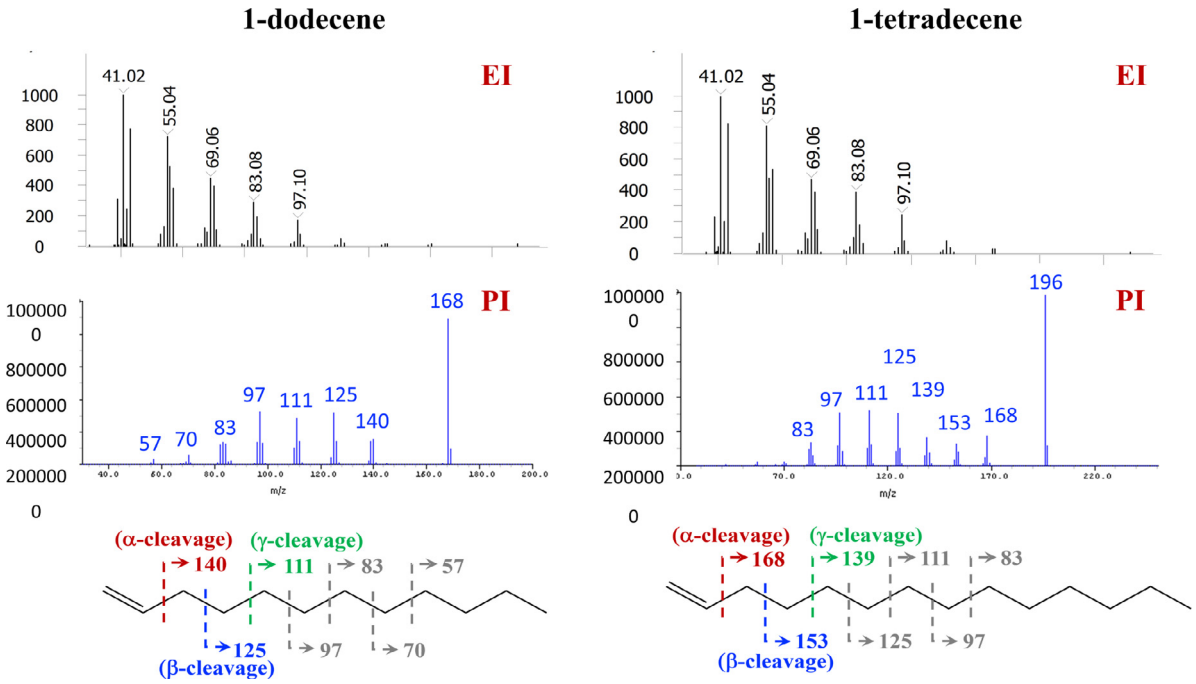


**Fig. 2.** Comparison between EI and PI mass spectra of 1-dodecene and 1-tetradecene.

also presented different fragment patterns in PI mass spectra. Comparing to EI mass spectra, the signals of fragments *m/z* 97, 111, 125, 140 in 1-dodecene (nominal mass of 168 Da) and *m/z* 97, 111, 125, 139, 153, 168 in 1-tetradecene (nominal mass of 196 Da) were enhanced in PI mass spectra. Smaller *m/z* fragments did not show high intensities in PI (Fig. 2). The relatively high abundance of *m/z* 125 in 1-dodecene and *m/z* 153 in 1-tetradecene were contributed by the allylic cleavage (the cleavage of allylic bond, which is between $\alpha$-C and $\beta$-C). It was reported that the allylic cleavage is the most dominant fragmentation pathway of olefins (carbon chain length $\leq$ 9) in PI, which could be valuable for determining the double bond location in the olefin [19,21]. The vinylic cleavage (the cleavage of vinylic bond, which is between the vinyl group and $\alpha$-C) was observed in 2-alkenes, but not commonly observed in 1-alkenes among shorter chain olefins [18]. In this study, fragments *m/z* 140 and 168 in 1-dodecene and 1-tetradecene, were attributed to vinylic cleavage with a loss of $C_2H_4$ (*m/z* 28). Moreover, the intensity of *m/z* 168 was slightly higher than *m/z* 153 in 1-tetradecene, which indicated that vinylic cleavage was as common as allylic cleavage in longer chain olefins. In addition, the cleavage of the bond between $\beta$-C and $\gamma$-C ($\gamma$-bond-cleavage hereinafter) was observed in 1-dodecene and 1-tetradecene as proved by *m/z* 111 and 139, respectively. This result is consistent with the work of Van Bramer and co-workers who observed $\gamma$-bond-cleavage in all 1-alkenes [18]. Interestingly, vinylic cleavage fragments corresponded to $[M\text{-}C_nH_{2n}]^{+\bullet}$ (*m/z* 140 and 168), but allylic cleavage and $\gamma$-bond-cleavage fragments corresponded to $[M\text{-}C_nH_{2n+1}]^{+}$ (*m/z* 125 and 111 in 1-dodecene, *m/z* 153 and 139 in 1-tetradecene). The observed $[M\text{-}C_nH_{2n+1}]^{+}$ could be explained by a secondary loss of $H_2$ from $[M\text{-}C_nH_{2n-1}]^{+}$ which was directly produced from allylic cleavage. Van Bramer also reported that the saturated radicals from larger alkenes often underwent the loss of $H_2$ in secondary fragmentation [18]. Most of the resulting fragments corresponded to $[M\text{-}C_nH_{2n+1}]^{+}$, except for *m/z* 70 and 57 in 1-dodecene corresponding to $[M\text{-}C_nH_{2n}]^{+\bullet}$ and $[M\text{-}C_nH_{2n-1}]^{+}$, respectively (Fig. 2). The advantage of PI on the isomer structure prediction, together with the enhanced separation power by GC×GC makes GC×GC-PI-TOFMS a more suitable and powerful tool to study the composition of dodecene products compared to traditional GC-EI-MS.

### 3.3. Olefin congener distribution

Utilizing the predominant intensity of molecular ions in PI mass spectra, olefin congeners were grouped by carbon chain length and DBE. Most of the dodecene samples (see Table S1) evaluated consisted $C_{9\text{-}15}$ (DBE = 1) and $C_{11\text{-}13}$ (DBE = 2) congeners. $C_8$, $C_{16}$, $C_{18}$ (DBE = 1) and $C_{10}$, $C_{14}$, $C_{15}$ (DBE = 2) contributed negligibly (< 0.06%). Hydro GC showed no significant presence of cyclic-alkanes or cyclic-alkenes (SI S-4). Therefore, a DBE of 1 and 2 in this study indicated monoolefins and diolefins, respectively. The dominant congener group was dodecene, contributing 62.32 – 90.17% among the evaluated samples. The second abundant congener group was undecene contributing up to 29.46%. Sample J, for example, also consisted of relatively abundant shorter olefins, nonene and decene, at 16.47% and 10.16%, respectively. The fraction of diolefin, however, was much lower, below 2.17% among the evaluated samples (Fig. 3a,b). Although the production process was the same, the olefin congener distribution among the evaluated samples showed large difference. This variation cannot be solely explained by neither the feeds nor the catalysts. Therefore, an insight into the dodecene structural subgroup distribution was conducted among the samples.

### 3.4. Dodecene subgroup distribution

BI is a measure of the average branching. It is calculated from wt% of mono-, di-, and tri-branched subgroups within the same carbon chain length. Details of the calculation are given in (SI S-5). Data for the BI calculation were obtained by hydro GC under the assumption that the retention time (RT) of linear, mono-, di- and tri-branched subgroups had no overlap. Due to the uncertainty of separation between di- and tri-branched subgroups by hydro GC, the sum of these two groups were grouped, and an average of 2.5 was used for the number of branches in this combined group. Based on the same assumption, the $^1t_R$ boundaries

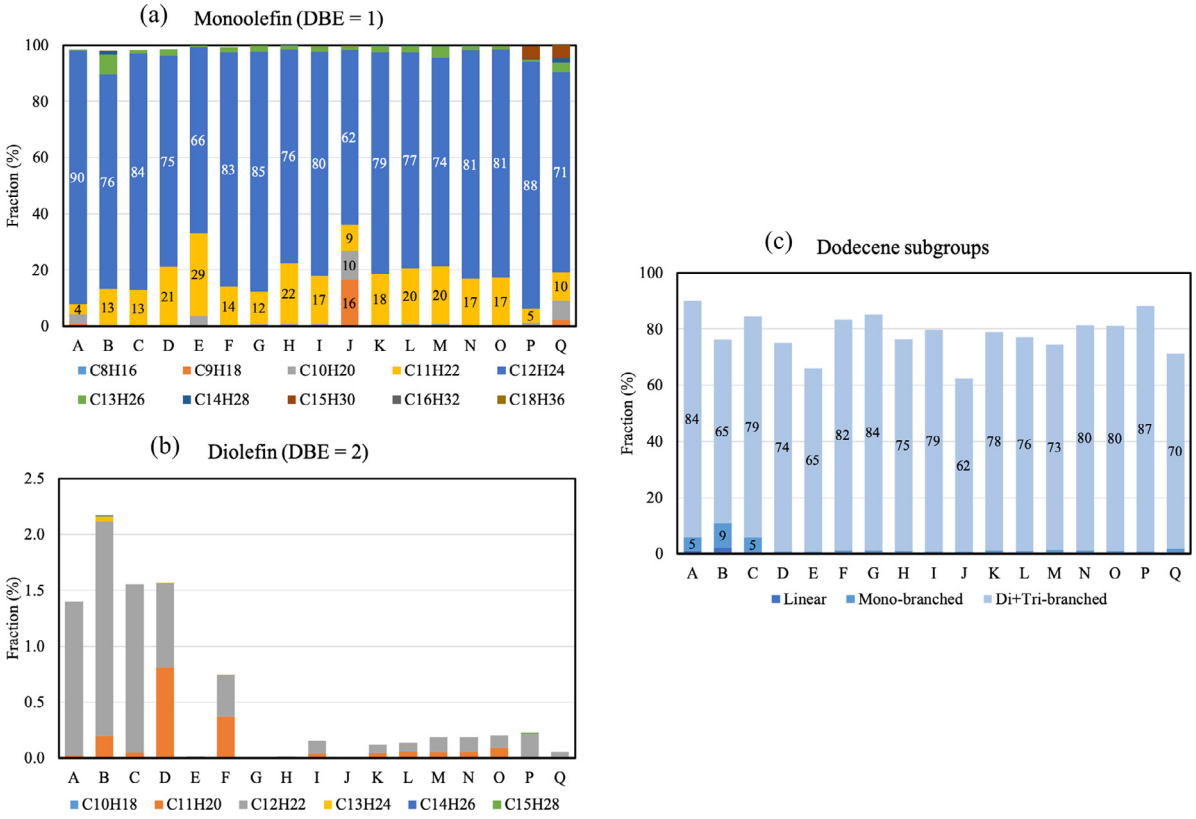


**Fig. 3.** The percent distributions of monoolefins (a), diolefins (b), and dodecene subgroups (c) in commercial dodecene products.

between linear, mono-branched, and di+tri-branched subgroups of dodecene were estimated by the wt% data from hydro GC and peak volumes from GC×GC-PI-TOFMS. The predicted $^1t_R$ boundary between linear and mono-branched subgroups was 54.3 min. The boundary between mono-branched and di+tri-branched subgroups was 50.3 min. Accordingly, the fractions of dodecene subgroups in dodecene samples were calculated (Fig. 3c). Di+tri-branched isomers were predominantly present, contributing 62 – 87% to the products. Whereas mono-branched and linear dodecene isomers showed relatively low or neglectable contributions.

### *3.5. Structural identification of linear dodecene isomers based on PI spectra*

RI is a robust parameter for identifying isomers. Kovats' RI on the non-polar column OV-101 is the only data set in the NIST Chemistry WebBook we can refer to containing eleven linear dodecene isomers [24]. Since the reference RI data were obtained under isothermal condition, the absolute value of reference RI could not be directly compared with the RI in our work. However, the difference in RI between two neighboring isomers (ΔRI) may be used for isomer identification (Table S6, S7).

The BI-reference-sample contained more linear dodecene isomers than the dodecene samples. Nine peaks were detected within linear dodecene $^1t_R$ boundary (Fig. 4). According to ΔRI, peaks 4 – 9 were predicted as (E)-5-dodecene, (E)-4-dodecene, (Z)-4-dodecene, (Z)-3-dodecene, (E)-2-dodecene and (Z)-2-dodecene, respectively. To be specific, the ΔRI between peaks 8 and 9 was 9.2, which matched to the value of 9 of the ΔRI between (Z)-2-dodecene and (E)-2-dodecene in the reference. The ΔRI between peaks 7 and 8 was 7.6, which was close to ΔRI of 7 between (E)-2-dodecene and (Z)-3-dodecene in the reference (Table S6, S7, Fig. 4). The structures of peaks 4 – 6 were predicted likewise. However, ΔRI between peaks 1 – 3 did not match to reference. Therefore, they may not be linear dodecenes, but mono-branched isomers (Table S6, S7, Fig. 4).

In peak 4, the fragments *m/z* 125 and 97 were the allylic radicals produced by allylic cleavage (Fig. 4). It is reported that the predominant fragment in linear olefins is allylic radical produced by allylic cleavage. The reason is that the cleavage at the $\beta$ C-C bond to produce an allylic radical requires less energy than fragmentation at other locations [18]. Moreover, the allylic radicals are less likely than allylic radical cations to undergo H atom rearrangement prior to ionic fragmentation. This is because the radical cations have lower rearrangement barriers than the neutral precursors [18]. Therefore, the abundance of fragments *m/z* 123 and 95 was much lower than m/z 125 and 97. Van Bramer and coworkers illustrated that neutral fragmentation occurs without significant isomerization in PDPI-MS, which further enabled structural isomer identification [18]. Besides allylic cleavage, vinylic cleavage also occurred and was shown by the presence of the corresponding fragments, *m/z* 111 and 83, in peak 4. However, the abundance of vinylic cleavage fragments was lower than allylic cleavage fragments, which is consistent with the report of Van Bramer and coworkers [18]. They also observed that vinylic cleavage fragments were less abundant than allylic cleavage fragments in 2-, 3-, and 4-alkenes. Moreover, in 1-alkenes $\gamma$−bond-cleavage was observed as well [18]. The significant intensity of *m/z* 139 in peak 4 illustrated the occurrence of $\gamma$−bond-cleavage in (E)-5-dodecene.

Peaks 5 and 6 are assigned to (E)-4-dodecene and (Z)-4-dodecene respectively. The second most abundant fragment besides the molecular ion was *m/z* 139 in both mass spectra (Fig. 4). This fragment was produced from allylic cleavage, which indicated the double bond location. The other allylic cleavage produced allylic radical was *m/z* 83 (Fig. 4). *m/z* 125 was a vinylic cleavage product. The other vinylic cleavage produced a saturated radical,

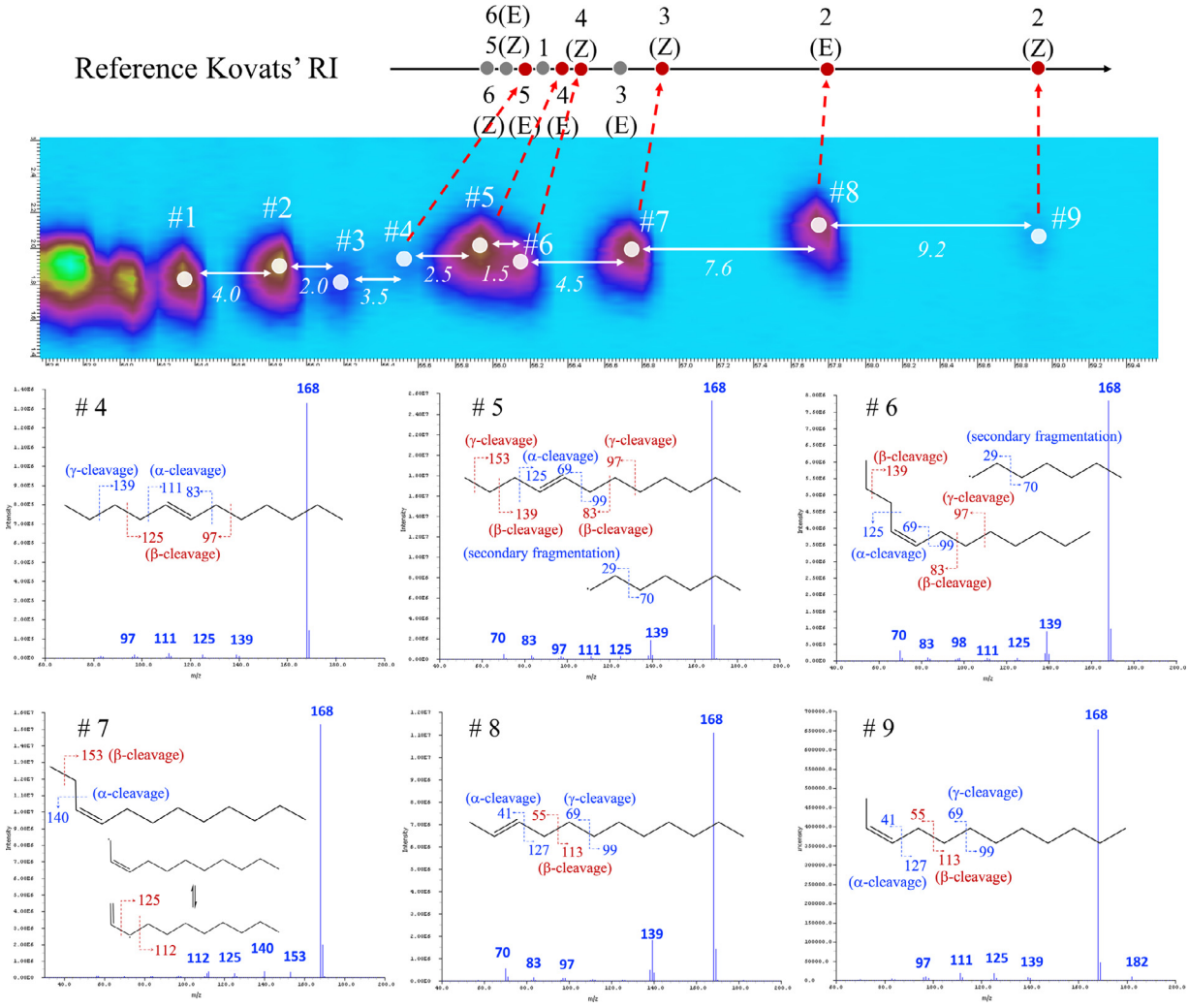


**Fig. 4.** The structural identification of linear dodecene isomers of BI-reference-sample by Kovats' RI and PI mass spectra. The presented structures are predicted structures. $\alpha$-cleavage and $\beta$-cleavage in this figure mean vinylic cleavage and allylic cleavage, respectively, in the text. $\gamma$-cleavage in this figure means $\gamma$-bond-cleavage in the text.

*m/z* 99. It subsequently underwent neutral secondary fragmentation and produced $C_2H_5^\bullet$ (*m/z* 29) and $C_5H_{10}$ (*m/z* 70). $\gamma$−bond-cleavage took place and presented *m/z* 97. In peak 6, the allylic radical $C_{10}H_{19}^\bullet$ (*m/z* 139) formed by allylic cleavage firstly underwent a double bond and radical shift, then a subsequent McLafferty rearrangement resulting in $C_3H_5^\bullet$ (*m/z* 41) and $C_7H_{14}$ (*m/z* 98) (Fig. S3).

The appearance of fragment *m/z* 153 in peak 7 suggested a double bond locating between the 3rd and 4th C. A part of the *m/z* 153 fragments reacted further with a double bond shift and a McLafferty rearrangement. This explained the presence of $C_3H_5^\bullet$ (*m/z* 41) and $C_8H_{16}$ (*m/z* 112) in the mass spectrum (Fig. S3). Another part of the *m/z* 153 fragment underwent a free radical delocalization, followed by vinylic cleavage producing *m/z* 125. The fragment of *m/z* 140 was generated from vinylic cleavage between 2nd and 3rd C of original molecule.

Peaks 8 and 9 are identified as 2-dodecene isomers. High abundance of *m/z* 125, 111, and 97 in peak 9 can be explained by the loss of $H_2$ of the saturated radicals $C_9H_{19}^\bullet$ (*m/z* 127), $C_8H_{17}^\bullet$ (*m/z* 113), and $C_7H_{15}^\bullet$ (*m/z* 99) from vinylic, allylic and $\gamma$−bond-cleavage, respectively (Fig. S3). This is because the saturated radicals in larger alkenes often undergo a secondary loss of $H_2$ [18]. In peak 8, secondary fragmentation of saturated radicals $C_9H_{19}^\bullet$ (*m/z* 127) and $C_8H_{17}^\bullet$ (*m/z* 113) produced $C_7H_{15}^\bullet$ (*m/z* 99) and $C_6H_{13}^\bullet$ (*m/z* 85). This is followed by a loss of $H_2$ producing *m/z* 97 and 83 fragments. The secondary fragmentation of radical $C_7H_{15}^\bullet$ (*m/z* 99) by $\gamma$−bond-cleavage produced $C_5H_{10}$ (*m/z* 70). The production of fragment *m/z* 139 might be explained by several subsequent steps. First, $C_{11}H_{21}^\bullet$ (*m/z* 153) was produced by an initial vinylic cleavage. Then, the free radical was stabilized by resonance and double bond isomerization. Eventually, another vinylic cleavage produced $C_{10}H_{19}^\bullet$ (*m/z* 139) (Fig. S3). The above structural identifications of linear dodecene isomers were based on the PI spectra and RI. Further experiments are needed to verify the exact chemical structures by standard compounds.

### 3.6. Structural identification of branched dodecene isomers based on PI spectra

The mass spectra of peaks 1 – 3 which are in the linear dodecene zone did not show the expected allylic cleavage fragments of 5-dodecene (*m/z* 125) and 6-dodecene (*m/z* 111). Therefore, they may not be linear dodecenes, but mono-branched isomers (Fig. S4). RI references are very limited for branched-dodecene isomers in NIST Chemistry WebBook. Hence, PI mass spectra were applied for structure identification. In ionization and fragmentation of branched isomers, expect for vinylic, allylic and $\gamma$−bond-cleavage, secondary fragmentation also took place [18]. The pre-

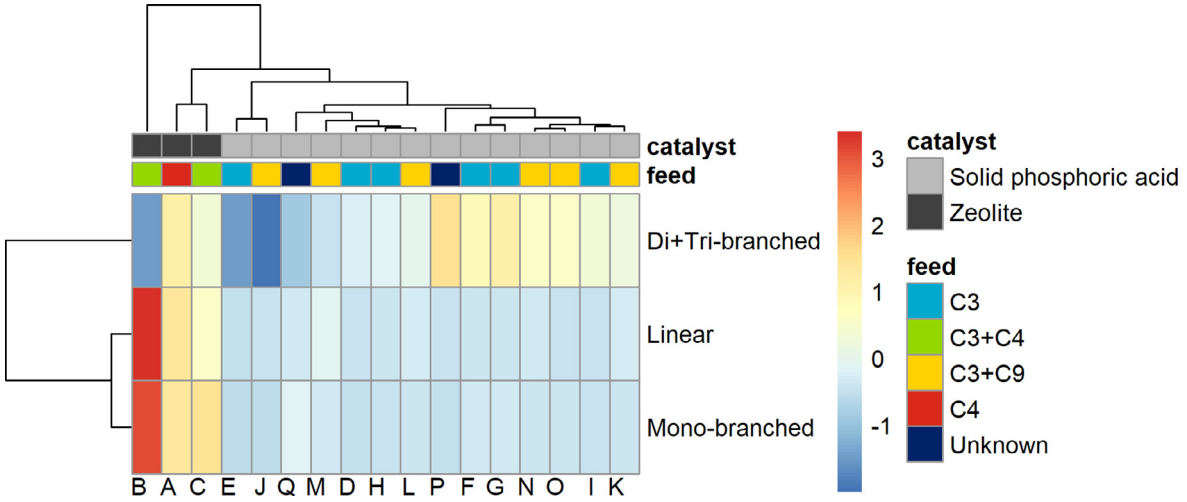


**Fig. 5.** Heat map of seventeen dodecene products based on percent distribution of dodecene subgroups.

dicted structures of peaks 1 – 3 are 5-ethyl-5-decene, 6-methyl-4-undecene, and 3-methyl-4-undecene, respectively (Fig. S4). In peak 1, *m/z* 125 fragment indicated the first allylic cleavage and the double bond location. The *m/z* 84 fragment is the result of a secondary allylic cleavage of the allylic radical *m/z* 125. In peak 2, first a allylic cleavage produced allylic radicals with *m/z* 153, 139, and 97. The allylic radicals underwent a secondary allylic cleavage and produced fragments with *m/z* 125, 84, and 70. In peak 3, the second most abundant fragment *m/z* 139 was obtained by allylic cleavage. This is also the case for the fragments with *m/z* 153 and 98. Secondary allylic cleavage resulted in fragments with *m/z* 125 and 84. The fragment with *m/z* 112 was from secondary vinylic cleavage (Fig. S4). Based on all of these data, the $^1t_R$ boundary between linear and mono-branched subgroups was re-defined as 55.2 min.

Some mono-branched isomers which eluted between 50.3 and 54.3 min were assigned to 8-methyl-2-undecene, 9-methyl-5-undecene, 8-methyl-5-undecen, 8-methyl-4-undecene, and 9-methyl-4-undecene, respectively (Fig. S5). The structural identifications described in this section were based on PI spectra and very limited reference of RI. Therefore, confirmation by the standard compounds will be needed in the future study. Due to the lack of RI references and the high complexity of isomer structures, the identification of di- and tri-branched isomers was not carried out in this study.

### 3.7. Statistical characterization of dodecene products

The olefin congener distribution and dodecene subgroup distribution of seventeen dodecene samples were determined by the optimized analytical condition. Heat map (distance method: Euclidean; clustering method: average-linkage) and PCA based on the dodecene subgroup distribution well separated dodecene products by different catalysts as well as feeds (Fig. 5 and S6). In catalyst aspect of view, sample A, B, and C produced by zeolite were higher in linear and mono-branched isomers than the other samples produced by solid phosphoric acid. To the effect of feed composition, $C_4$ and $C_3$+$C_4$ produced dodecene products were with higher level of linear and mono-branched isomers compared to the feeds without $C_4$. Sample A, which was produced using the $C_4$ feed, was higher in di+tri-branched isomers than sample B and C which were from a $C_3$+$C_4$ feed. The feeds used to produce samples P and Q were unknown. However, the samples were distanced from samples A – C in heat map, which indicated less probability that they were obtained from a $C_4$ containing feed. Moreover, samples K, L, M, N, O were produced by adding nonene into samples H and I which were obtained by a $C_3$ only feed. In the heat map samples K, O, N were clustered together with their precursor sample I, and samples L and M were grouped with the other precursor sample H (Fig. 5).

Since samples A, B, and C were produced using zeolite catalyst, were also the ones produced by the feeds containing $C_4$ olefins, but PCA cannot tell which is the differentiating factor for the samples: catalyst type or feed composition. Therefore, a one-way and two-way ANOVA were conducted. Taking feed (4 levels: $C_3$, $C_3$+$C_4$, $C_4$ and $C_3$+$C_9$) and catalyst (2 levels: zeolite and solid phosphoric acid) as independent variables, and the percent distribution of mono-branched isomer as dependent variable, we found a statistically significant difference in the percent distribution of mono-branched isomers by both feed ($p < 0.01$) and catalyst ($p < 0.01$) in one-way ANOVA. However, the difference was significant only in the impact of catalyst type on the percent distribution of mono-branched isomers in two-way ANOVA. Using the Akaike information criterion (AIC) the one-way ANOVA (catalyst) was the model that best explained the variation in the percent distribution of mono-branched isomers. This model could explain 93% of the variation.

## 4. Conclusions

The fingerprint chromatogram of olefin mixtures was successfully obtained by GC×GC-PI-TOFMS. This study highlighted the combination of GC×GC and PI-TOFMS as a state-of-the art approach for detailed molecular characterization of ultra-complex samples, such as olefin mixtures. The global information of olefin congeners and isomers and statistical analyses solved the challenge of differentiating various dodecene products and elucidated the impact of feed and catalyst on the product composition. Due to the lack of olefin isomer mono-standards and limited reference RI, some dodecene isomers could not be identified in this study. The PI ionization and fragmentation mechanisms will be better resolved if more olefin standards are available. Moreover, a PI mass spectra simulation based on physicochemical parameters such as ionization energy and appearance energy of possible fragments is also worth developing in a future study especially in the absence of standards.

Supporting Information

S-1. The sample information (Table S1. The feed and catalyst summary of seventeen dodecene products); S-2. Details of analytical condition (Table S2. The optimized condition of GC×GC-PI-TOFMS; Table S3. The analytical condition of Hydro GC); S-3. Frac-

tional factorial experimental design (DoE) (Table S4. Three factor – three level DoE for reversed (polar × nonpolar) column set; Figure S1. Main effect plots of DoE for reversed (polar × nonpolar) column set; Table S5. Three factor – three level DoE for conventional (nonpolar × polar) column set; Figure S2. Main effect plots of DoE for conventional (nonpolar × polar) column set); S-4. Determination of cyclic hydrocarbons; S-5. The calculation of branching index (BI); S-6. Kovats' retention index (RI) of linear dodecene isomers (Table S6. The reference Kovats' RI of linear dodecene isomers from NIST Chemistry WebBook; Table S7. The Kovats' RI of potential linear dodecene isomers in BI-reference-sample); S-7. The fragmentation mechanism schemes of linear dodecene isomers (Figure S3. The fragmentation mechanism schemes of (E)-2-dodecene, (Z)-2-dodecene, (Z)-3-dodecene and (Z)-4-dodecene); S-8. The chromatograms and PI mass spectra of mono-branched dodecene isomers (Figure S4. The chromatograms and PI mass spectra of peaks 1 – 3 falling in linear dodecene isomer zone; Figure S5. The chromatograms and PI mass spectra of peaks 1 – 5 falling in mono-branched isomer zone); S-9. PCA score and loading plots of seventeen dodecene products (Figure S6. PCA score and loading plots of seventeen dodecene products. PCA scores were grouped by feed and catalyst, respectively).

## Declaration of Competing Interest

The authors declare that they have no known competing financial interests or personal relationships that could have appeared to influence the work reported in this paper.

## CRediT authorship contribution statement

**Yun Zou:** Methodology, Software, Validation, Formal analysis, Investigation, Writing - original draft, Writing - review & editing, Visualization. **Pierre-Hugues Stefanuto:** Methodology, Data curation, Writing - review & editing. **Mariarosa Maimone:** Resources, Writing - review & editing, Funding acquisition. **Marcel Janssen:** Resources, Writing - review & editing, Funding acquisition. **Jean-François Focant:** Conceptualization, Resources, Writing - review & editing, Supervision, Project administration, Funding acquisition.

## Acknowledgment

The authors thank JEOL Ltd., J&X Technologies, and Leco Corporation for the support on instrumentation. Thanks are also given to Dr. Flavio A. Franchina for suggestion and discussion on the method optimization, and Dr. Shan Niu for discussion on the method of statistical analysis. This work was supported by ExxonMobil Chemical Europe Inc.

## Supplementary materials

Supplementary material associated with this article can be found, in the online version, at doi:10.1016/j.chroma.2021.462103.

## References

[1] E. Kriván, S. Tomasek, J. Hancsók, Application possibilities of zeolite catalysts in oligomerization of light olefins, Period. Polytech. Chem. Eng. 58 (2014) 149–156, doi:10.3311/PPch.7204.

[2] A. Giri, M. Coutriade, A. Racaud, K. Okuda, J. Dane, R.B. Cody, J.F. Focant, Molecular Characterization of Volatiles and Petrochemical Base Oils by Photo-Ionization GC×GC-TOF-MS, Anal. Chem. 89 (2017) 5395–5403, doi:10.1021/acs.analchem.7b00124.

[3] C.M. Reddy, R.K. Nelson, S.P. Sylva, L. Xu, E.A. Peacock, B. Raghuraman, O.C. Mullins, Identification and quantification of alkene-based drilling fluids in crude oils by comprehensive two-dimensional gas chromatography with flame ionization detection, J. Chromatogr. A. 1148 (2007) 100–107, doi:10.1016/j.chroma.2007.03.001.

[4] M.S. Alam, C. Stark, R.M. Harrison, Using Variable Ionization Energy Time-of-Flight Mass Spectrometry with Comprehensive GC×GC to Identify Isomeric Species, Anal. Chem. 88 (2016) 4211–4220, doi:10.1021/acs.analchem.5b03122.

[5] A. Giri, M. Coutriade, A. Racaud, P.H. Stefanuto, K. Okuda, J. Dane, R.B. Cody, J.F. Focant, Compositional elucidation of heavy petroleum base oil by GC × GC-EI/PI/CI/FI-TOFMS, J. Mass Spectrom. 54 (2019) 148–157, doi:10.1002/jms.4319.

[6] M.S. Eschner, W. Welthagen, T.M. Gröger, M. Gonin, K. Fuhrer, R. Zimmermann, Comprehensive multidimensional separation methods by hyphenation of single-photon ionization time-of-flight mass spectrometry (SPI-TOF-MS) with GC and GC×GC, Anal. Bioanal. Chem. 398 (2010) 1435–1445, doi:10.1007/s00216-010-4021-0.

[7] U. Keshet, A.B. Fialkov, T. Alon, A. Amirav, A New Pulsed Flow Modulation GC × GC–MS with Cold EI System and Its Application for Jet Fuel Analysis, Chromatographia 79 (2016) 741–754, doi:10.1007/s10337-016-3087-z.

[8] B. Munson, Development of chemical ionization mass spectrometry, Int. J. Mass Spectrom. 200 (2000) 243–251, doi:10.1016/S1387-3806(00)00301-8.

[9] M.S.B. Munson, F.H. Field, Chemical Ionization Mass Spectrometry. I. General Introduction, J. Am. Chem. Soc. 88 (1966) 2621–2630, doi:10.1021/ja00964a001.

[10] T. Murata, S. Takahashi, Qualitative and quantitative chemical ionization mass spectrometry of triglycerides, Anal. Chem. 49 (1977) 728–731, doi:10.1021/ac50014a016.

[11] H.D. Beckey, Determination of the Structures of Organic Molecules and Quantitative Analyses with the Field Ionization Mass Spectrometer, Angew. Chemie Int. Ed. English. (1969), doi:10.1002/anie.196906231.

[12] C. Fenselau, S.Y. Wang, P. Brown, Field ionization mass spectra of photopolymers of thymine, Tetrahedron 26 (1970) 5923–5927, doi:10.1016/0040-4020(70)80029-1.

[13] R.P. Lattimer, H.-R. Schulten, FIELD IONIZATION AND FIELD DESORPTION MASS SPECTROMETRY: PAST, PRESENT, AND FUTURE, Anal. Chem. 61 (1989) 1201A–1215A, doi:10.1021/ac00196a721.

[14] L. Hanley, R. Zimmermann, Light and molecular ions: The emergence of vacuum UV single-photon ionization in MS, Anal. Chem. 81 (2009) 4174–4182, doi:10.1021/ac8013675.

[15] U. Boesl, Multiphoton excitation and mass-selective ion detection for neutral and ion spectroscopy, J. Phys. Chem. 95 (1991) 2949–2962, doi:10.1021/j100161a005.

[16] R. Bekker, N.M. Prinsloo, Butene oligomerization over phosphoric acid: Structural characterization of products, Ind. Eng. Chem. Res. 48 (2009) 10156–10162, doi:10.1021/ie900210q.

[17] O. Ramnäs, U. Östermark, G. Petersson, Characterization of sixty alkenes in a cat-cracked gasoline naphtha by gas chromatography, Chromatographia 38 (1994) 222–226, doi:10.1007/BF02290340.

[18] S.E. Van Bramer, P.L. Ross, M.V Johnston, Unimolecular Photochemistry of n-Alkenes Studied by Photodissociation-Photoionization Mass Spectrometry, J. Am. Soc. Mass Spectrom. 4 (1993) 65–72.

[19] Scott E. Van Bramer; Murray, V. Johnston, Photodissociation-Photoionization Mass Spectrometry of, Anal. Chem. 62 (1990) 2643–2646.

[20] S.E. Van Bramer, M.V. Johnston, 10.5-eV photoionization mass spectrometry of aliphatic compounds, J. Am. Soc. Mass Spectrom. 1 (1990) 419–426, doi:10.1016/1044-0305(90)85024-G.

[21] Scott E. Van Bramer; Murray, V. Johnston, 18_Bramer and Johnston, 1992. structural identification of alkene. photodissociation-photoionization.pdf, Org. Mass Spectrom. 27 (1992) 949–954.

[22] Katriena Elizabet van der Westhuizen, Comprehensive multidimensional gas chromatography for the analysis of Fischer-Tropsch products, 2011.

[23] R. van der Westhuizen, H. Potgieter, N. Prinsloo, A. de Villiers, P. Sandra, Fractionation by liquid chromatography combined with comprehensive two-dimensional gas chromatography-mass spectrometry for analysis of cyclics in oligomerisation products of Fischer-Tropsch derived light alkenes, J. Chromatogr. A. 1218 (2011) 3173–3179, doi:10.1016/j.chroma.2010.10.009.

[24] S. Rang, K. Kuningas, T. Strenze, A. Orav, O. Eisen, Retention and thermodynamics of solution of n-alkenes in OV-101, J. Chromatogr. A. 406 (1987) 75–80, doi:10.1016/S0021-9673(00)94018-4.